

Publisher: GSA  
Journal: GEOL: Geology  
DOI:10.1130/G38216.1

1 Inside baleen: Exceptional microstructure preservation in a  
2 late Miocene whale skeleton from Peru

3 **Anna Gioncada<sup>1</sup>, Alberto Collareta<sup>1,2</sup>, Karen Gariboldi<sup>1,2</sup>, Olivier Lambert<sup>3</sup>,**

4 **Claudio Di Celma<sup>4</sup>, Elena Bonaccorsi<sup>1</sup>, Mario Urbina<sup>5</sup>, and Giovanni Bianucci<sup>1</sup>**

5 *<sup>1</sup>Dipartimento di Scienze della Terra, Università di Pisa, via S. Maria 53, 56126 Pisa,*

6 *Italy*

7 *<sup>2</sup>Dottorato Regionale in Scienze della Terra Pegaso, via S. Maria 53, 56126 Pisa, Italy*

8 *<sup>3</sup>Institut Royal des Sciences Naturelles de Belgique, D.O. Terre et Histoire de la Vie, rue*

9 *Vautier 29, 1000 Brussels, Belgium*

10 *<sup>4</sup>Scuola di Scienze e Tecnologia, Università di Camerino, via Gentile III da Varano,*

11 *62032 Camerino, Italy*

12 *<sup>5</sup>Departamento de Paleontología de Vertebrados, Museo de Historia Natural de la*

13 *Universidad Nacional Mayor de San Marcos, Avenida Arenales 1256, Lima 14, Peru*

14 E-Mail Addresses: [anna.gioncada@unipi.it](mailto:anna.gioncada@unipi.it), [elena.bonaccorsi@unipi.it](mailto:elena.bonaccorsi@unipi.it),

15 [giovanni.bianucci@unipi.it](mailto:giovanni.bianucci@unipi.it), [alberto.collareta@for.unipi.it](mailto:alberto.collareta@for.unipi.it), [karen.gariboldi@for.unipi.it](mailto:karen.gariboldi@for.unipi.it),

16 [olivier.lambert@naturalsciences.be](mailto:olivier.lambert@naturalsciences.be), [claudio.dicelma@unicam.it](mailto:claudio.dicelma@unicam.it),

17 [mariourbina01@hotmail.com](mailto:mariourbina01@hotmail.com)

18 **ABSTRACT**

19 Exceptionally preserved delicate baleen microstructures have been found in  
20 association with the skeleton of a late Miocene balaenopteroid whale in a dolomite  
21 concretion of the Pisco Formation, Peru. Microanalytical data (scanning electron  
22 microscopy, electron probe microanalysis, X-ray diffraction) on fossil baleen are

23 provided and the results are discussed in terms of their taphonomic and paleoecological  
24 implications. Baleen fossilization modes at this site include molding of plates and  
25 tubules, and phosphatization. A rapid formation of the concretion was fundamental for  
26 fossilization. We suggest that the whale foundered in a soft sediment chemically  
27 favorable to rapid dolomite precipitation, allowing the preservation of delicate structures.  
28 Morphometric considerations on the baleen plates and bristles coupled with the  
29 reconstructed calcification of the latter permit speculation on the trophic preferences of  
30 this balaenopteroid whale: the densely-spaced plates and the fine and calcified bristles  
31 provide evidence for feeding on small-sized plankton, as the modern sei whale.

## 32 **INTRODUCTION**

33         Despite the long and relatively diversified fossil record of baleen-bearing whales  
34 (originating ca 34 Ma ago; see Deméré et al., 2008; Marx and Fordyce, 2015), the  
35 preservation of baleen structures in situ is extremely rare (e.g., Packard, 1946; Barnes et  
36 al., 1987). This sparse fossil record is due to the more rapid decomposition of baleen  
37 (formed of keratin and minor hydroxyapatite, Fig. 1A) as compared to bone, and to the  
38 detachment of baleen racks from maxillae following the decay of epithelial tissues.  
39 Nevertheless, in the Mio-Pliocene Pisco Formation (Peru), fossilized baleen racks have  
40 been described associated to several dozens of whale skeletons, strengthening the  
41 identification of the Pisco fossil deposits as a Lagerstätte (Pilleri and Pilleri, 1989; Brand  
42 et al., 2004; Esperante et al., 2008; Bisconti, 2012).

43         We describe the exceptional finding of a fossil balaenopteroid whale skeleton  
44 with preserved baleen in a dolomite concretion from the Pisco Fm, and interpret the fossil  
45 structures through a microanalytical study of the remains, aimed at (i) understanding the

46 modes of fossilization and (ii) reconstructing the original characteristics of the baleen.  
47 Furthermore, our observations allow us to infer the trophic habits of the studied fossil  
48 balaenopteroid.

#### 49 **FIELD DESCRIPTION**

50 The 200 m-thick section of the Pisco Fm exposed at Cerro Colorado (CC  
51 hereafter, Fig. 1B) has been recently assigned to the early late Miocene (Tortonian, ca 9  
52 Ma) based on new biostratigraphic and tephrochronological data (Di Celma et al., 2016).  
53 The CC site is overwhelmingly rich in marine fossil vertebrates, including mysticetes as  
54 well as the holotype of the giant raptorial sperm whale *Livyatan melvillei* (Bianucci et al.,  
55 2010, 2016, Lambert et al., 2010, 2015, Collareta et al., 2015).

56 In September 2014, a partial skeleton of a mysticete whale was discovered  
57 (14°21'13.4"S – 75°53'0.1"W) embedded within a layer of diatomaceous silts in the  
58 upper portion of the Pisco Fm lower allomember (DR1). The skeleton (M1 in the CC  
59 fossil vertebrates map of Bianucci et al., 2016) consists of the skull, both mandibles, both  
60 baleen racks (Fig. 1C, D), and portions of the postcranial skeleton (vertebrae, ribs, and  
61 forelimbs) enclosed in a hard dolomitic concretion. Despite weathering having caused  
62 this concretion to break into several pieces, observations on the parts still preserved in  
63 situ indicate that M1 settled and fossilized dorsal-side up. The degree of articulation of  
64 M1 is remarkably high; there is no evidence of diagenetic compaction and, except for a  
65 moderate degree of recent weathering on exposed bony surfaces, its preservation is  
66 excellent. Observations and measurements in the field (DR2) allowed referring M1 to a  
67 young adult of the undescribed middle-sized balaenopteroid species recognized at CC by  
68 Collareta et al. (2015).

69           The right baleen rack is preserved between the medial surface of the right  
70 mandible and the right ventrolateral margin of the vomer (Fig. 1D). This rack is  
71 apparently complete and fully articulated; it is composed of 2–5 mm thick and regularly  
72 spaced plate-like structures, with the spaces in between encrusted by gypsum. We  
73 counted 20 plates in a length of 10 cm measured parallel to the long axis of the skull. The  
74 baleen rack is not preserved in life position; its base is detached from the lateral margin  
75 of the palate and is located along the ventral maxilla-vomer suture, due to a  
76 counterclockwise (in posterior view) rotation of ca 90°, exposing the ventral end of the  
77 plates near the labial edge of the maxilla. Anterior and posterior surfaces of the plates  
78 present thin, parallel grooves, rarely overlapping (Fig. 1E). Light-colored, string-like  
79 structures along the medial face of the mandible strongly resemble bristle remains (Fig.  
80 1F, G).

81           The left baleen rack is associated to the ventral surface of the left maxilla (Fig.  
82 1C). Based on the location of the supposed bristles near the medial edge of the maxilla,  
83 we hypothesize that, after deposition, the baleen plates rotated under the weight of the  
84 head of the mysticete (thus causing the bristles to touch the palatal face of the maxilla  
85 until its suture with the vomer).

86           Small pieces of the concretion with plate-like and bristle-like structures were  
87 sampled from fragments crumbled by natural erosion and deposited in the collection of  
88 the Museo de Historia Natural de la Universidad Nacional Mayor de San Marcos  
89 (MUSM), in Lima (collection number MUSM 3238). Some were prepared for scanning  
90 electron microscopy (SEM), electron probe microanalysis (EPMA), and X-ray diffraction  
91 analyses (methodological details in DR3).

92 **MICROANALYTICAL RESULTS**

93           The grooves along the surfaces of the plate-like structures are < 100 micron deep  
94 and have a semicircular cross section. Their morphology and position suggest that they  
95 are natural casts of baleen tubules. The plate-like structures do not show any internal  
96 circular feature reminiscent of tubules, and consist of terrigenous particles and diatom  
97 frustules in a dolomite cement (Fig. 2A).

98           The sediment containing bristles is constituted by diatom frustules thoroughly  
99 cemented by microcrystalline dolomite. The diatom frustules are slightly dislocated but  
100 not deformed by diagenetic compression (Fig. 2B), and show perfect preservation of  
101 silica ultrastructures (DR3). The sediment contains biogenic phosphatic fragments carved  
102 by microborings, the latter being filled by iron-bearing framboids (Fig. 2C).

103           When freed from the enclosing sediment, the objects we interpret as fragments of  
104 bristles consist of dolomite rods wrapped in an exfoliating material strongly resembling  
105 the arrangement of the epithelial cells of bristles (Pfeiffer, 1992) (Fig. 2D, F). Upon  
106 sectioning, the bristles show the inner lumen completely filled with dolomite, and the  
107 “walls” consisting of Ca-phosphate with layered structure (Fig. 2F). The peaks  
108 characteristic of fluorapatite are visible in X-ray diffraction spectra of the fossil bristle  
109 material, and the major element composition determined by EPMA corresponds to F-  
110 bearing apatite (see DR3 for data). As in the diatom frustules, the bristles are fragmented  
111 and displaced but the section of tubules is not deformed by compaction.

112 **DISCUSSION**

113           The plate-like structures of the fossil baleen racks are composed of a sediment  
114 framework cemented by dolomite and display casts of the baleen tubules only along the

115 outer surfaces. This confirms that these structures represent natural casts of the spaces  
116 between adjacent baleen plates in a rack, preserved thanks to the formation of the  
117 concretion. Their sediment framework indicates that the gaps between adjacent baleen  
118 plates - which, in the living whale, are maintained because the plates are regularly set  
119 within a soft tissue made of keratin (Fudge et al., 2009; Young et al., 2015) - were filled  
120 by sediment as soon as the whale settled along the sea bottom, before the start of keratin  
121 decay. Such a process would only be possible if the sea bottom was a soft sediment  
122 allowing the carcass to sink (Martill, 1993; Gariboldi et al., 2015), as supported by the  
123 high degree of articulation of the skeleton.

124         But, if the keratinous plates decayed away, how did the keratinous tubules survive  
125 long enough to leave their permanent imprint in the concretion? The answer comes from  
126 the free bristles we found inside the concretion. The 3D morphology of the bristle  
127 fragments is incredibly regular thanks to dolomite filling the medullary lumen (Fig. 2).  
128 Although the phosphatic material forming what remains of the cuticle of the tubules is  
129 now soft and erodible, the concretion holds a perfect imprint of this cuticle. This suggests  
130 that the tubules underwent a different decay and fossilization process than the keratin  
131 matrix of the baleen plates. Szewciw et al. (2010) showed that there is an uneven  
132 distribution of hydroxyapatite in the baleen of extant mysticetes, with strong interspecific  
133 differences: intertubular calcification prevails in the minke whale (*Balaenoptera*  
134 *acutorostrata*), whereas tubule calcification prevails in the sei whale (*Balaenoptera*  
135 *borealis*) and the humpback whale (*Megaptera novaeangliae*). The highest measured  
136 values of hydroxyapatite are recorded in the bristles of sei whale (14.5% dry weight;  
137 Pautard, 1963). Based on these observations, we propose that the baleen of the

138 balaenopteroid from CC were characterized by uneven calcification, with a higher  
139 concentration of apatite in the tubules. The higher calcification of the tubules may have  
140 stiffened them, so that they persisted even after the keratin of the plate matrix decayed  
141 away and left their imprints at the surface of the casts of the plates.

142         The “walls” of bristles have been replaced by fluorapatite, with a layered  
143 arrangement. Despite the porous appearance, it is unlikely that the observed Ca-  
144 phosphate is provided only by the original calcium salt crystallites. The fluorapatite  
145 could, instead, indicate a process of phosphate precipitation from seawater  
146 (phosphatization, e.g., Schiffbauer et al., 2014). The layered arrangement (Fig. 2F),  
147 recalling the annular distribution of calcification (Pautard, 1965; Szewciw et al., 2010),  
148 permits to infer that the original hydroxyapatite crystallites acted as nucleation sites for  
149 mineralization.

150         The rapid decrease of permeability related to the formation of the concretion is a  
151 main preservation factor (McCoy et al., 2015a, b). All evidence suggests early formation  
152 of the concretion, before the deformation by compaction of the fragile diatom frustules  
153 and before the obliteration by decay of the three-dimensional morphology of keratinous  
154 structures (Long and Trinajstic, 2010). However, as indicated by the low degree of  
155 phosphatization of bristle walls, the concretion formation may also have impeded further  
156 mineralization of the tubule structure.

157         Both the precipitation of dolomite for the concretion and the mechanism of  
158 phosphatization require an alkaline environment. A favorable alkaline environment was  
159 most likely induced by the decay of the whale’s organic matter, allowing early carbonate  
160 precipitation (e.g., Allison, 1988; Yoshida et al., 2015). In the concretion enclosing M1,

161 evidence for biomediated sulfate reduction (the relics of pyrite framboids in  
162 microborings, Fig. 2C) indicate conditions favorable for dolomite primary precipitation,  
163 as proposed for other dolomite concretions hosting vertebrate remains in CC (Gariboldi et  
164 al., 2015 and references therein). It cannot be excluded that the whale fell in a soft  
165 sediment layer close to the conditions for sulfate reduction, i.e., already rich in decaying  
166 organic matter.

167         Since in extant whales the calcification pattern of tubules is correlated to prey  
168 types, with mechanically strong, fine bristles corresponding to smaller prey (Szewciw et  
169 al., 2010), we can propose a similar correlation for M1. This is further supported by (i)  
170 the mean diameter of the baleen bristles in M1, which is low compared to most extant  
171 mysticetes (especially among Balaenopteroidea), and is similar to values reported by  
172 Young (2012) for the sei whale and the pygmy right whale (*Caperea marginata*), and by  
173 (ii) the relatively high plate density, comparable to densities observed in these two  
174 modern species. Both the sei and the pygmy right whale are currently known to feed  
175 mostly on small planktonic crustaceans (copepods) (see Young, 2012, and references  
176 therein). Interestingly, copepods are also the target prey of the Pacific pilchard *Sardinops*;  
177 the latter was abundant along the southern coast of Peru during the early late Miocene  
178 and occupied a prominent position in trophic chains of the CC vertebrate fauna (Lambert  
179 et al., 2015; Collareta et al., 2015). Therefore, we speculate that the middle-sized  
180 balaenopteroid species of CC represented by the specimen M1 fed predominantly on  
181 small-sized plankton, and more specifically on copepods.

182 **CONCLUSIONS**



183           Baleen fossilization modes in a balenopteroid specimen of the Pisco Fm include i)  
184 molding of baleen plates in a dolomite concretion, with imprints of the medullary tubules,  
185 and of bristles; ii) phosphatization of bristles favored by the same alkaline environment  
186 allowing dolomite formation. Possibly favored by sinking of the whale in a soft sediment  
187 layer chemically prone to dolomite precipitation, rapid formation of the concretion in  
188 respect to decay is testified by the lack of compression of the diatomaceous sediment and  
189 by the preservation of the delicate baleen structures.

190           The preservation of the casts of medullary tubules and bristles requires that decay  
191 of the tubules was delayed in respect to decay of the keratin matrix, suggesting a higher  
192 calcification of the tubules as compared to the intertubular keratin in the mysticete  
193 studied here. Based on the calcification of bristles, their diameter in the lower range of  
194 extant mysticetes and the high baleen plate density, we propose that this middle-sized  
195 balaenopteroid species fed predominantly on small-sized zooplankton, as the modern sei  
196 whale and the pygmy right whale.

#### 197 **ACKNOWLEDGMENTS**

198           The authors thank K. Post and B. Ramassamy who took part in the finding of the  
199 fossil specimen. W. Aguirre, F. Colarieti, R. Salas-Gismondi, M. J. Laime-Molina, and  
200 R. Varas-Malca are thanked for field and laboratory assistance. Reviews by A. Berta,  
201 R.W. Boessenecker, S. Dominici and anonymous are acknowledged. Research funded by  
202 PRIN 2012YJSBMK EAR-9317031, National Geographic Society 9410–13 and  
203 University of Pisa PRA\_2015\_0028.

#### 204 **REFERENCES CITED**

- 205 Allison, P.A., 1988, The role of anoxia in the decay and mineralization of proteinaceous  
206 macro-fossils: *Paleobiology*, v. 14, p. 139–154, doi:10.1017/S009483730001188X.
- 207 Barnes, L.G., Raschke, R.E., and Brown, J.C., 1987, A fossil baleen whale:  
208 *Whalewatcher*, v. 21, p. 7–10.
- 209 Bianucci, G., Lambert, O., and Post, K., 2010, High concentration of longsnouted beaked  
210 whales (genus *Messapicetus*) from the Miocene of Peru: *Palaeontology*, v. 53,  
211 p. 1077–1098, doi:10.1111/j.1475-4983.2010.00995.x.
- 212 Bianucci, G., Celma, C., Landini, W., Post, K., Tinelli, C., de Muizon, C., Gariboldi, K.,  
213 Malinverno, E., Cantalamessa, G., Gioncada, A., Collareta, A., Gismondi, R., Varas-  
214 Malca, R., Urbina, M., and Lambert, O., 2016, Mapping and vertical distribution of  
215 fossil marine vertebrates in Cerro Colorado, the type locality of the giant raptorial  
216 sperm whale *Livyatan melvillei* (Miocene, Pisco Formation, Peru): *Journal of Maps*,  
217 v. 12, p. 543–557, doi:10.1080/17445647.2015.1048315.
- 218 Bisconti, M., 2012, Comparative osteology and phylogenetic relationships of *Miocaperea*  
219 *pulchra*, the first fossil pygmy right whale genus and species (Cetacea, Mysticeti,  
220 Neobalaenidae): *Zoological Journal of the Linnean Society*, v. 166, p. 876–911,  
221 doi:10.1111/j.1096-3642.2012.00862.x.
- 222 Brand, L.R., Esperante, R., Chadwick, A.V., Poma-Porrás, O., and Alomia, M., 2004,  
223 Fossil whale preservation implies high diatom accumulation rate in the Miocene-  
224 Pliocene Pisco Formation of Peru: *Geology*, v. 32, p. 165–168,  
225 doi:10.1130/G20079.1.
- 226 Collareta, A., Landini, W., Lambert, O., Post, K., Tinelli, C., Di Celma, C., Panetta, D.,  
227 Tripodi, M., Salvadori, P.A., Caramella, D., Marchi, D., Urbina, M., and Bianucci,

- 228 G., 2015, Piscivory in a Miocene Cetotheriidae of Peru: First record of fossilized  
229 stomach content for an extinct baleen-bearing whale: *The Science of Nature*, v. 102,  
230 doi:10.1007/s00114-015-1319-y.
- 231 Deméré, T., McGowen, M., Berta, A., and Gatesy, J., 2008, Morphological and  
232 molecular evidence for a stepwise evolutionary transition from teeth to baleen in  
233 mysticete whales: *Systematic Biology*, v. 57, p. 15–37,  
234 doi:10.1080/10635150701884632.
- 235 Di Celma, C., Malinverno, E., Gariboldi, K., Gioncada, A., Rustichelli, A., Pierantoni, P.,  
236 Landini, W., Bosio, G., Tinelli, C., and Bianucci, G., 2016, Stratigraphic framework  
237 of the late Miocene to Pliocene Pisco Formation at Cerro Colorado (Ica Desert,  
238 Peru): *Journal of Maps*, v. 12, p. 515–529, doi:10.1080/17445647.2015.1047906.
- 239 Esperante, R., Brand, L., Nick, K., Poma-Porras, O., and Urbina, M., 2008, Exceptional  
240 occurrence of fossil baleen in shallow marine sediments of the Neogene Pisco  
241 Formation, Southern Peru: *Palaeogeography, Palaeoclimatology, Palaeoecology*,  
242 v. 257, p. 344–360, doi:10.1016/j.palaeo.2007.11.001.
- 243 Fudge, D.S., Szewciw, L.J., and Schwalb, A.N., 2009, Morphology and development of  
244 blue whale baleen: An annotated translation of Tycho Tullberg's classic 1883 paper:  
245 *Aquatic Mammals*, v. 35, p. 226–252, doi:10.1578/AM.35.2.2009.226.
- 246 Gariboldi, K., Gioncada, A., Bosio, G., Malinverno, G., Di Celma, C., Tinelli, C.,  
247 Cantalamessa, G., Landini, W., Urbina, M., and Bianucci, G., 2015, The dolomite  
248 nodules enclosing fossil marine vertebrates in the East Pisco Basin, Peru: Field and  
249 petrographic insights into the Lagerstätte formation: *Palaeogeography,*

- 250 Palaeoclimatology, Palaeoecology, v. 438, p. 81–95,  
251 doi:10.1016/j.palaeo.2015.07.047.
- 252 Lambert, O., Bianucci, G., Post, K., de Muizon, C., Salas-Gismondi, R., Urbina, M., and  
253 Reumer, J., 2010, The giant bite of a new raptorial sperm whale from the Miocene  
254 epoch of Peru: *Nature*, v. 466, p. 105–108, doi:10.1038/nature09067.
- 255 Lambert, O., Collareta, A., Landini, W., Post, K., Ramassamy, B., Di Celma, C., Urbina,  
256 M., and Bianucci, G., 2015, No deep diving: evidence of predation on epipelagic fish  
257 for a stem beaked whale from the late Miocene of Peru: *Proceedings of the Royal*  
258 *Society of London Part B: Biological Sciences*, v. 282, doi:10.1098/rspb.2015.1530.
- 259 Long, J.A., and Trinajstić, K., 2010, The Late Devonian Gogo Formation lagerstätte of  
260 Western Australia: Exceptional early vertebrate preservation and diversity: *Annual*  
261 *Review of Earth and Planetary Sciences*, v. 38, p. 255–279, doi:10.1146/annurev-  
262 earth-040809-152416.
- 263 Martill, D.M., 1993, Soupy substrates: a medium for the exceptional preservation of  
264 ichthyosaurs of the Posidonia Shale (Lower Jurassic) of Germany: *Kaupia*, v. 2,  
265 p. 77–97.
- 266 Marx, F.G., and Fordyce, R.E., 2015, Baleen boom and bust: a synthesis of mysticete  
267 phylogeny, diversity and disparity: *Royal Society Open Science*, v. 2,  
268 doi:10.1098/rsos.140434.
- 269 McCoy, V.E., Young, R.T., and Briggs, D.E.G., 2015a, Factors controlling exceptional  
270 preservation in concretions: *Palaios*, v. 30, p. 272–280, doi:10.2110/palo.2014.081.

- 271 McCoy, V.E., Young, R.T., and Briggs, D.E.G., 2015b, Sediment permeability and the  
272 preservation of soft-tissues in concretions: an experimental study: *Palaios*, v. 30,  
273 p. 608–612, doi:10.2110/palo.2015.002.
- 274 Packard, E.L., 1946, Fossil baleen from the Pliocene of Cape Blanco, Oregon: Oregon  
275 State College: *Studies in Geology (Tulsa)*, v. 5, p. 3–11.
- 276 Pautard, F.G.E., 1963, Mineralization of keratin and its comparison with the enamel  
277 matrix: *Nature*, v. 199, p. 531–535, doi:10.1038/199531a0.
- 278 Pautard, F.G.E., 1965, Calcification of baleen, in Richella, L.J., and Dallemagne, M.J.,  
279 eds., *Calcified tissues: Proceedings of the Third European Symposium on Calcified*  
280 *Tissues held at Davos*, p. 347–357.
- 281 Pfeiffer, C.J., 1992, Cellular structure of terminal baleen in various mysticete species:  
282 *Aquatic Mammals*, v. 18, p. 67–73.
- 283 Pilleri, G., and Pilleri, O., 1989, *Balaenoptera siberi*, ein neuer balaenopterid (Cetacea)  
284 aus der Pisco-Formation Perus I. Beitrage zur Palaeontologie der Cetaceen Perus I:  
285 Switzerland, Hirnanatomisches Institut der Universitat Bern Ostermundigen, p. 63–  
286 106.
- 287 Schiffbauer, J.D., Wallace, A.F., Broce, J., and Xiao, S., 2014, Exceptional fossil  
288 conservation through phosphatization: *The Paleontological Society Papers*, v. 20,  
289 p. 59–82.
- 290 Szewciw, L.J., De Kerckhove, D.G., Grime, G.W., and Fudge, D.S., 2010, Calcification  
291 provides mechanical reinforcement to whale baleen  $\alpha$ -keratin: *Proceedings of the*  
292 *Royal Society of London Part B: Biological Sciences*, v. 277, p. 2597–2605,  
293 doi:10.1098/rspb.2010.0399.

- 294 Yoshida, H., Ujihara, A., Minami, M., Asahara, Y., Katsuta, N., Yamamoto, K., Sirono,  
295 S., Maruyama, I., Nishimoto, S., and Metcalfe, R., 2015, Early post-mortem  
296 formation of carbonate concretions around tusk-shells over week-month timescales:  
297 Scientific Reports, v. 5, doi:10.1038/srep14123.
- 298 Young, S., 2012, The comparative anatomy of baleen: Evolutionary and ecological  
299 implications [M.Sc. Thesis]: San Diego, San Diego State University, 122 p.
- 300 Young, S., Deméré, T.A., Ekdale, E.G., Berta, A., and Zellmer, N., 2015, Morphometrics  
301 and structure of complete baleen racks in gray whales (*Eschrichtius robustus*) from  
302 the eastern North Pacific Ocean: The Anatomical Record, v. 298, p. 703–719,  
303 doi:10.1002/ar.23108.

304

305 FIGURE CAPTIONS

306

- 307 Figure 1. A. Main baleen features of an extant rorqual, at different scales; tubules  
308 diameter is on the order of 0.5 mm (modified and redrawn from Szewciw et al., 2010). B.  
309 Location of Cerro Colorado (see detailed map in DR1). C, D. The right (D) and left (C)  
310 baleen racks of the balaenopteroid M1 as found in the field, with drawings showing their  
311 original position in the whale skull. Dolomite = dolomite concretion. E. Surface of plate-  
312 like structure with tubule casts (arrow) in specimen M1. F. Fossil bristles of specimen M1  
313 at the end of plates. G. The same as in F, in extant balaenopterid baleen.

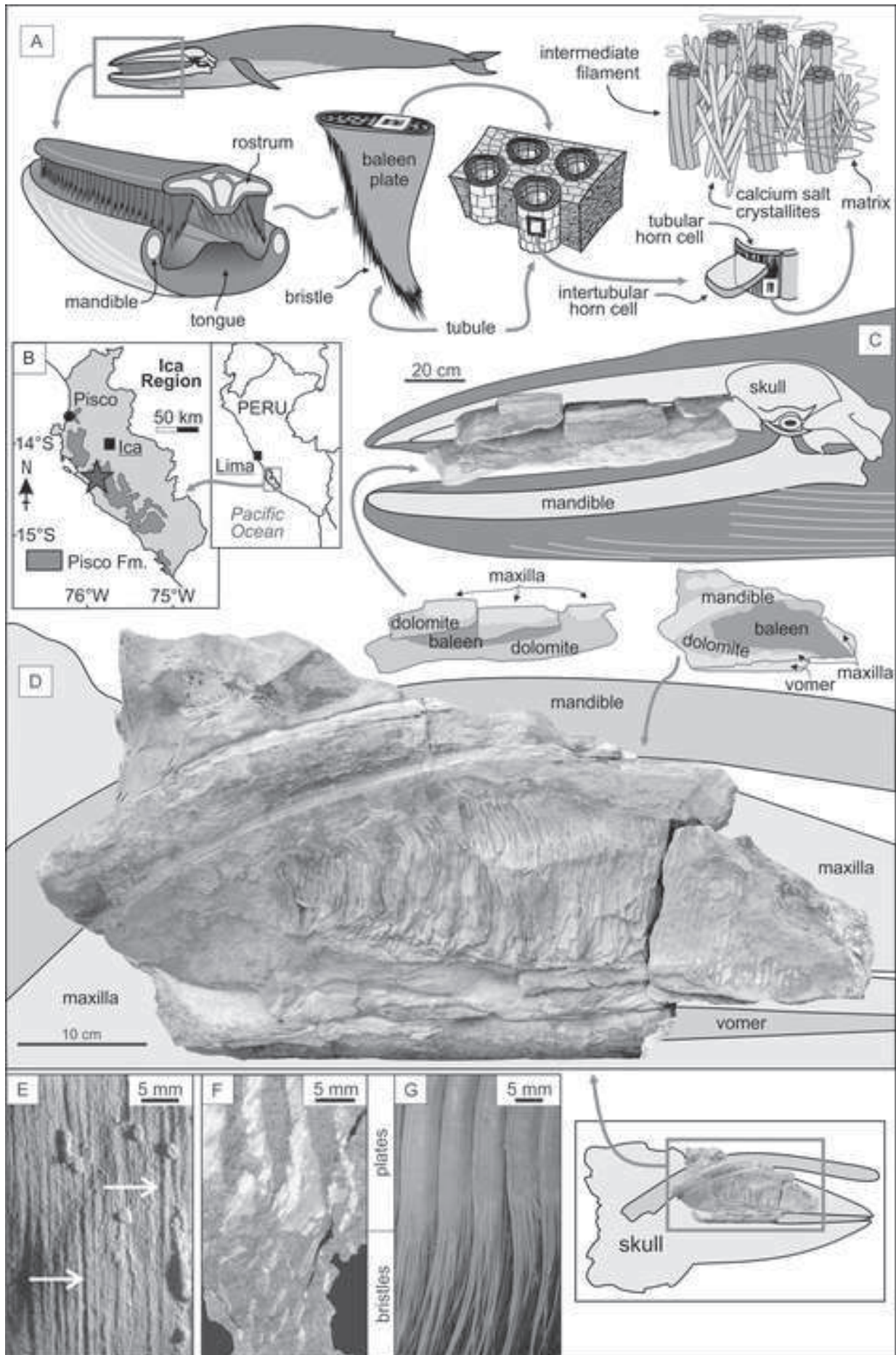
314

315 Figure 2. SEM images of the dolomite concretion (A, B), of framboids in microboring of  
316 phosphatic fragments (C), of fossil bristle fragments (D, E) and section (F).  
317 Backscattered electron images except D and E (secondary electron images).

318

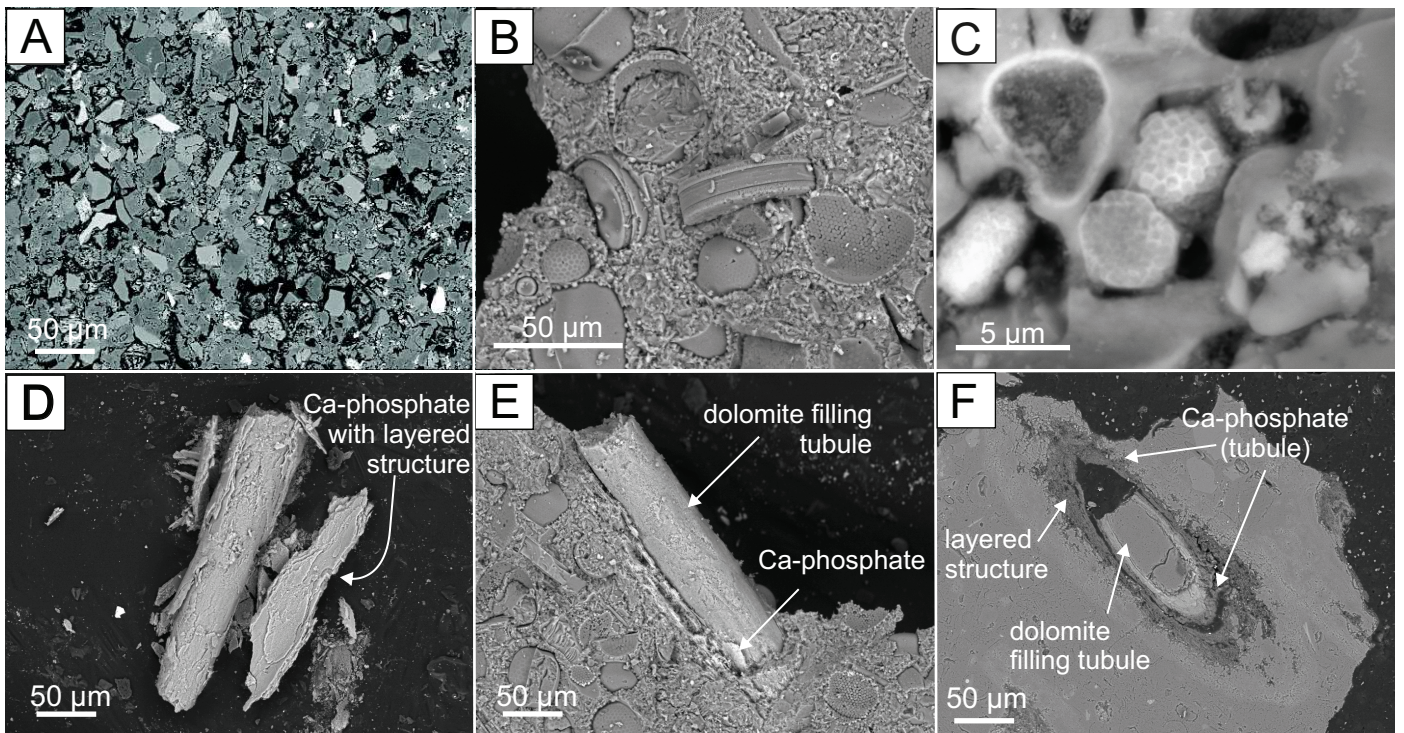
319 <sup>1</sup>GSA Data Repository item 201Xxxx, geological map and stratigraphic section,  
320 paleontological details, analytical details and data, is available online at

**300**





Gioncada et alii, Figure 2



## Gioncada et alii, DR1

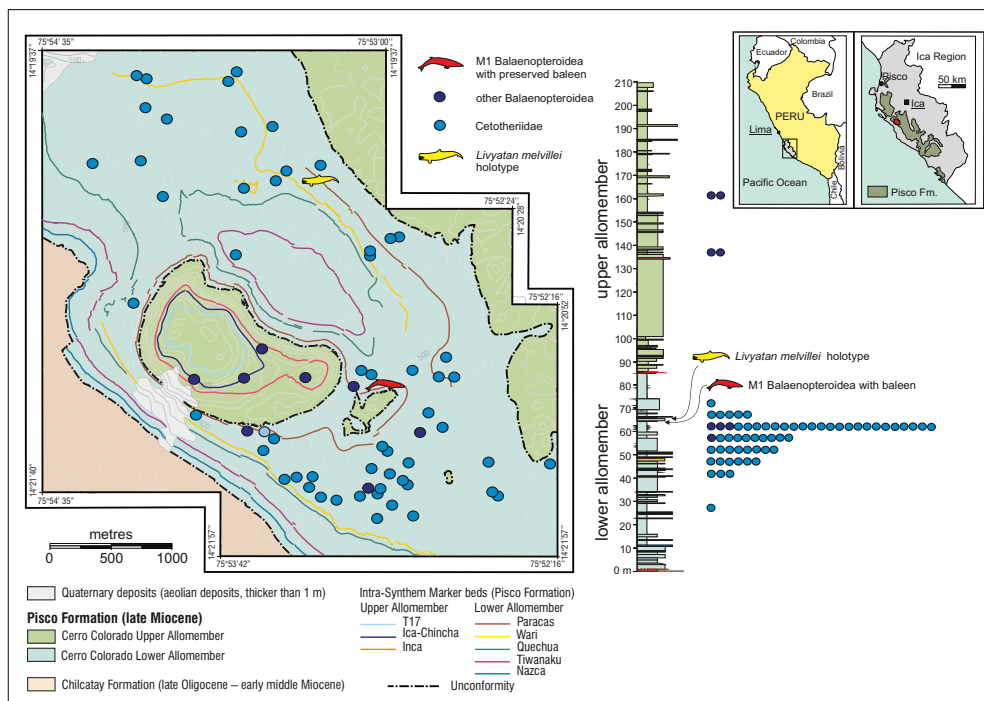


Figure DR1. Cerro Colorado geological map and stratigraphic section modified from Bianucci et al. (2016), showing the distribution of fossil mysticetes and the position of M1. The position of *Livyatan melvillei* holotype finding is also reported.

## Reference cited

Bianucci, G., Celma C., Landini W., Post K., Tinelli C., de Muizon C., Gariboldi K., Malinverno E., Cantalamessa G., Gioncada A., Collareta A., Gismondi R., Varas-Malca R., Urbina M. and Lambert O., 2016, Mapping and vertical distribution of fossil marine vertebrates in Cerro Colorado, the type locality of the giant raptorial sperm whale *Livyatan melvillei* (Miocene, Pisco Formation, Peru): Journal of Maps, v. 12, p. 543–557, doi:10.1080/17445647.2015.1048315.

Gioncada et alii, DR2. Additional paleontological observations on the balaenopteroid whale skeleton M1

M1 displays a high degree of articulation, e.g.: both mandibles are still in anatomic connection with the cranium; the forelimbs show perfectly articulated carpal and metacarpal bones; the exposed segment of vertebral column presents articulated vertebrae; the bony thorax (thoracic vertebrae and ribs) preserves its three-dimensional architecture (see figure below).

The skull, mandibles, and ear bones of M1, which are divided into several blocks and fragments, display a typically balaenopteroid outline. A bizygomatic width of ca 96 cm has been estimated for M1. This measurement allows calculating a total body length of ca 8.5 m based on the equation proposed by Lambert et al. (2010). Based on the presence of vertebral epiphyses ankylosed to the relative apophyses, M1 is regarded as a fully grown adult individual; as such, it is here attributed to the undescribed middle-sized (ca 7-9 m long) balaenopteroid species recognized at Cerro Colorado by Collareta et al. (2015).



Figure. The bony thorax (thoracic vertebrae and ribs) of M1 preserves its three-dimensional architecture attesting the high degree of articulation of the fossil mysticete skeleton (long dimension of the photo is about 1 m).

#### References cited

- Collareta, A., Landini W., Lambert O., Post K., Tinelli C., Di Celma C., Panetta D., Tripodi M., Salvadori P.A., Caramella D., Marchi D., Urbina M., Bianucci G., 2015, Piscivory in a Miocene Cetotheriidae of Peru: first record of fossilized stomach content for an extinct baleen-bearing whale: *The Science of Nature*, v. 102, article no. 70, doi:10.1007/s00114-015-1319-y.
- Lambert, O., Bianucci, G., Post, K., de Muizon, C., Salas-Gismondi, R., Urbina, M., and Reumer, J., 2010, The giant bite of a new raptorial sperm whale from the Miocene epoch of Peru: *Nature*, v. 466, p. 105–108, doi:10.1038/nature09067.

## DR3. Material preparation, analytical methods and data

### Material preparation and analytical methods

Small pieces of the concretion holding plate-like structures were mounted in resin and sectioned, orthogonally to and along the grooves; one fragment holding bristles was gently crushed to expose the delicate strings. Some phosphatic material was collected from the fossil bristles with a needle and powdered for X-rays diffraction analysis (XRPD). Some fragments were mounted in resin within tube-like holders and polished exposing a section of the string orthogonal to its long axis; others were mounted without resin. The mounts were carbon-coated for scanning electron microscopy with backscattered electrons imaging and energy-dispersive X-ray spectroscopy (SEM-EDS, Philips XL30 SEM equipped with DX4i EDAX microanalysis) and wavelength-dispersive spectroscopy electron probe microanalysis (WDS-EPMA, Cameca SX50 instrument at CNR, Rome, Italy). X-ray powder diffraction (XRPD) data were collected on a Bruker D2 Phaser diffractometer operating at 10 mA and 30 kV, using a flat background-free sample holder and Cu K $\alpha$  radiation with  $\lambda = 1.54178 \text{ \AA}$ . Data were processed using the software DIFFRAC.EVA V4.1.

### Data

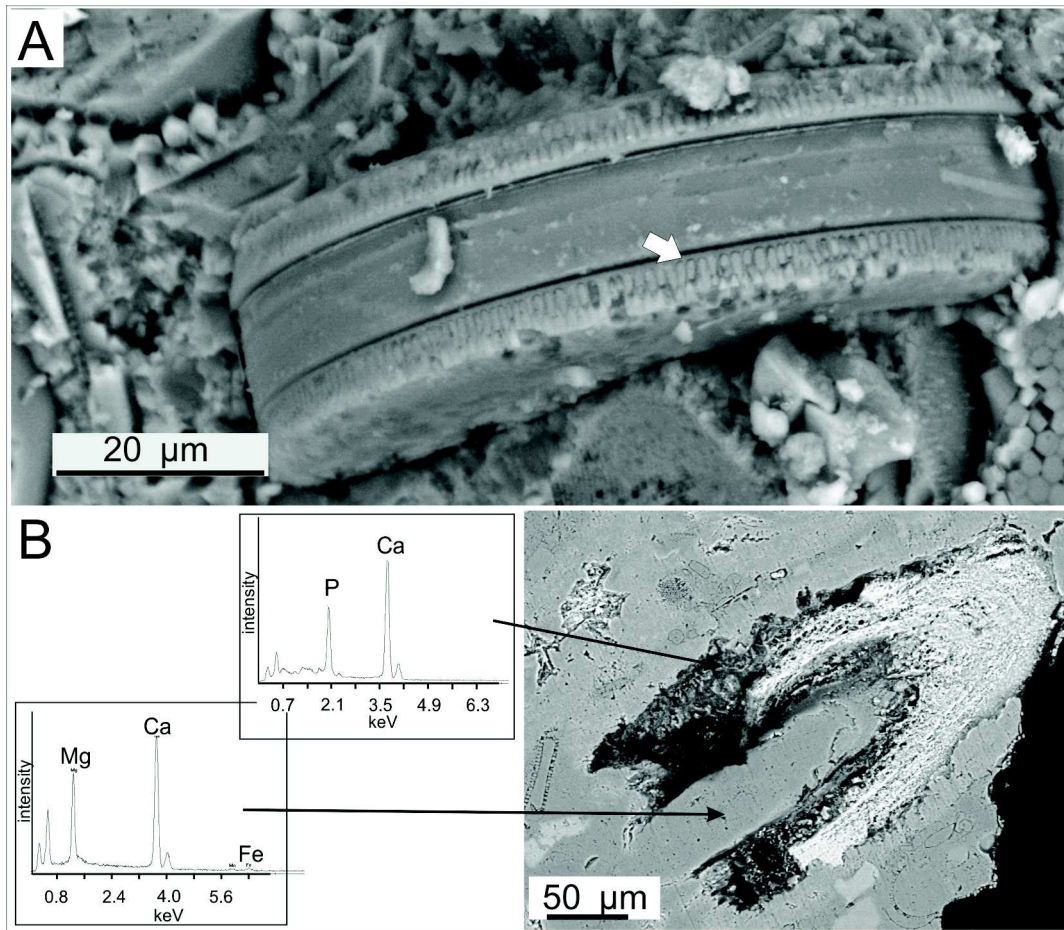
#### SEM-EDS

Through SEM-EDS analysis, the concretion forming the plates casts and containing fossil bristles was carefully investigated to identify the fossil evidence of tubules and their mineral composition. Analytical conditions were 20 kV accelerating voltage, 5 nA beam current.

The well cemented diatomaceous sediment encasing free bristles (Fig. 2b in the paper) has >95% of diatom frustules and minor terrigenous particles; 95% of the diatom assemblage is made of *Stephanopyxis* spp. and frustule outlines lack any indication of diagenetic compression. In the enlargement here below (A), *Azpeitia* sp. frustule can be recognized; silica is preserved and details of the frustules ultrastructure are still visible; white arrow indicates diamond-shaped areolae on the

mantle and no signs of diagenetic compression are found (SEM-SE). In B, an example of Ca-phosphate and dolomite identification by SEM in a sectioned fossil bristle is shown. The brighter area corresponds to Ca-phosphate permeated by late gypsum (SEM-BSE).

Figure DR3\_1

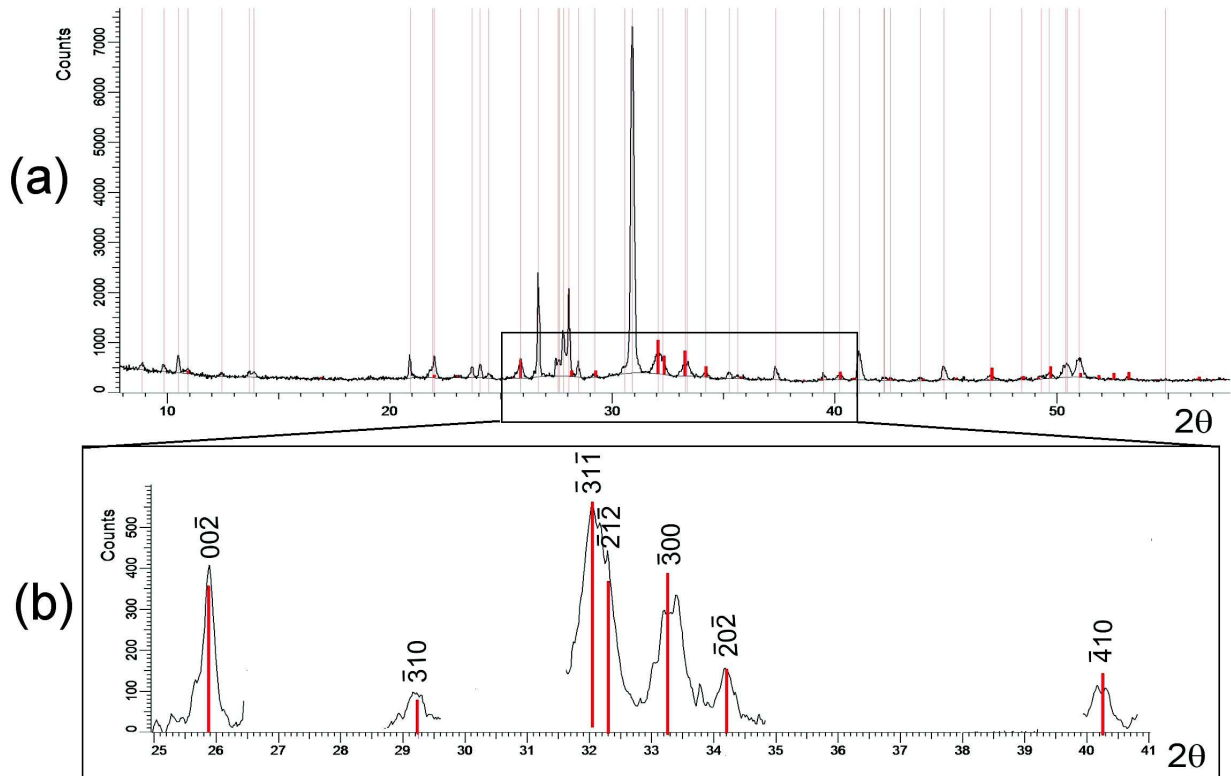


## X-rays DIFFRACTION

The sample was manually selected under binoculars. A preliminary X-ray diffraction powder (XRPD) pattern indicated that the occurring main phases were dolomite, gypsum and quartz. The same sample was gently ground in water; after two hours the water was removed and the sample was dried at 80°C in a furnace. The final XRPD pattern is reported in Figure DR3\_2(a); the identified phases were dolomite, quartz, minor amounts of orthopyroxenes, amphibole and plagioclase, and, as emphasized in Figure DR3\_2(b), apatite-(CaF) (‘fluorapatite’). In the enlarged portion of

the XRPD pattern, only the ‘fluorapatite’ peaks not superimposed to indexed peaks of other phases are reported.

Figure DR3\_2



## ELECTRON MICROPROBE

EPM analyses of Ca-phosphate of the bristles and of the dolomite are reported in Table DR3\_1 (below). The Ca-phosphate analyses give values for the Ca/P atomic ratio which are higher compared to hydroxyapatite composition (Wopenka and Pasteris, 2005), but in the range of published bioapatite bone materials (Li and Pasteris, 2014). The occurrence of low amounts of sulfur in analyses 1-4, joined to the relatively high Ca content, could be due to the pervasive occurrence of gypsum within porosity. We attribute the low totals of Ca-phosphate compared to published EMPA data (Li and Pasteris, 2014) to the imperfect surface obtained when polishing such porous material.

|                                    | Ca-phosphate |       |       |       | dolomite |       |       |       |
|------------------------------------|--------------|-------|-------|-------|----------|-------|-------|-------|
|                                    | 1            | 2     | 3     | 4     | 5        | 6     | 7     | 8     |
| wt%                                |              |       |       |       |          |       |       |       |
| SO <sub>3</sub>                    | 1.84         | 1.99  | 1.48  | 1.64  | 0.02     | bdl   | 0.03  | 0.06  |
| P <sub>2</sub> O <sub>5</sub>      | 31.28        | 31.42 | 30.38 | 31.94 | 0.06     | 0.09  | 0.12  | 0.18  |
| SiO <sub>2</sub>                   | 1.34         | 1.49  | 1.43  | 1.77  | 0.02     | bdl   | 0.06  | 0.01  |
| Fe <sub>2</sub> O <sub>3</sub> tot | 0.06         | 0.12  | 0.05  | 0.10  | 0.06     | 0.02  | 0.02  | 0.05  |
| MgO                                | 1.06         | 1.21  | 1.15  | 1.26  | 21.69    | 20.79 | 20.48 | 21.06 |
| CaO                                | 44.35        | 44.93 | 44.35 | 45.13 | 31.98    | 31.29 | 31.55 | 31.42 |
| MnO                                | 0.04         | 0.05  | 0.05  | 0.05  | 0.03     | 0.03  | bdl   | 0.05  |
| SrO                                | 0.14         | 0.30  | 0.16  | 0.15  | 0.13     | 0.15  | 0.01  | 0.14  |
| PbO                                | bdl          | bdl   | 0.03  | bdl   | 0.06     | bdl   | bdl   | 0.00  |
| Na <sub>2</sub> O                  | 0.90         | 1.01  | 0.95  | 0.91  | 0.07     | 0.09  | 0.04  | 0.08  |
| F                                  | 2.86         | 2.86  | 3.14  | 2.88  | 0.08     | bdl   | 0.08  | 0.01  |
| Cl                                 | 0.13         | 0.11  | 0.20  | 0.20  | 0.01     | 0.02  | 0.01  | 0.02  |
| sum                                | 84.01        | 85.48 | 83.34 | 86.02 | 54.20    | 52.47 | 52.40 | 53.06 |
| Ca/P atomic ratio                  | 1.80         | 1.81  | 1.85  | 1.79  |          |       |       |       |

Table DR3\_1. Electron probe WDS analyses of the phosphatic material now forming the bristles (1-4) and of the dolomite cementing the concretion (5-8); bdl: below detection limit; Fe<sub>2</sub>O<sub>3</sub>tot: all Fe as Fe<sub>2</sub>O<sub>3</sub>. Analytical conditions: 15kV accelerating voltage, 5 nA beam current. A 10 micron defocused beam was used.

#### References cited

Li, Z., Pasteris, J.D., 2014, Tracing the pathway of compositional changes in bone mineral with age: Preliminary study of bioapatite aging in hypermineralized dolphin's bulla: *Biochimica et Biophysica Acta*, v. 1840, p. 2331–2339.

Wopenka, B., Pasteris, J.D., 2005, A mineralogical perspective on the apatite in bone: *Materials Science and Engineering, C 25*, p.131–143.